Performance of periodic EOM-CCSD for band gaps of inorganic semiconductors and insulators

Ethan A. Vo,1 Xiao Wang,2 and Timothy C. Berkelbach1, a)

We calculate the band gaps of 12 inorganic semiconductors and insulators composed of atoms from the first three rows of the periodic table using periodic equation-of-motion coupled-cluster theory with single and double excitations (EOM-CCSD). Our calculations are performed with atom-centered triple-zeta basis sets and up to 64 k-points in the Brillouin zone. We analyze the convergence behavior with respect to number of orbitals and number of k-points sampled, using composite corrections and extrapolations to produce our final values. When accounting for electron-phonon corrections to experimental band gaps, we find that EOM-CCSD has a mean signed error of -0.12 eV and a mean absolute error of 0.42 eV; the largest outliers are C (error of -0.93 eV), BP (-1.00 eV), and LiH (+0.78 eV). Surprisingly, we find that the more affordable partitioned EOM-MP2 theory performs as well as EOM-CCSD.

I. INTRODUCTION

The accurate *ab initio* prediction of electronic band structures and band gaps is a major driving force behind the improvement and development of increasingly accurate electronic structure methods. The failures of local and semilocal density functional theory (DFT) for this task have long been understood, ^{1–3} motivating the use of various hybrid functionals. ^{4–6} In a many-body framework, the GW approximation to the self-energy ^{7–9} is arguably the most successful method on the basis of its good accuracy and relatively low computational cost, with technical issues and extensions such as self-consistency and vertex corrections continuing to be explored. ^{10–15}

In the last decade, wavefunction-based electronic structure methods have been increasingly applied to solids. Seven years ago, McClain *et al.* ¹⁶ performed the first calculation of band gaps of periodic three-dimensional solids using equation-of-motion coupled-cluster theory with single and double excitations (EOM-CCSD) for ionization potentials and electron affinities, presenting encouraging results for diamond and silicon. Since then, the method has been applied to select solids, including MnO, NiO, ¹⁷ MoS₂, ¹⁸ and ZnO, ¹⁹ and has been developed as an impurity solver for dynamical mean-field theory. ^{20–22} However, the statistical performance of the method over a wide range of solids has yet to be established. We note that EOM-CCSD has also been used to study the neutral excitation energies of bulk solids, in periodic^{23–25} and embedded cluster²⁶ frameworks, and defects. ^{27,28}

Here, we aim to conclude this first phase of exploratory work by presenting converged band gaps of 12 simple, canonical semiconductors and insulators composed of atoms from the first three rows of the periodic table. Importantly, this work benefits from recent infrastructure developments, including efficient calculation of periodic integrals and density fitting ^{29–31} and the development of Gaussian basis sets that can be reliably converged to the basis set limit in closely packed solids. ³² We hope that our results can help direct future re-

search on the use of wavefunction based methods for excitation energies of solids, such as applications to more complex solids or improvements to cost or accuracy.

II. METHODS

A. Materials

We study 12 semiconductors and insulators with a range of covalent and ionic bonding and diverse crystal structures, including diamond (C, Si), zinc blende (SiC, BN, BP, AlP), rock salt (MgO, MgS, LiH, LiF, LiCL), and wurtzite (AlN). Each contains two atoms per unit cell except for AlN, which contains four atoms per unit cell. We use the experimental lattice constants for all solids, which are given in Tab. I. For all solids, we use DFT with the PBE functional and a large *k*-point mesh to identify the points in the Brillouin zone where the valence band maximum and conduction band minimum occur.

B. EOM-CCSD calculations

Periodic EOM-CCSD calculations were performed using PySCF³³ with Gaussian density fitting of two-electron integrals.^{29–31} We perform a periodic Hartree-Fock calculation, then a ground-state CCSD calculation, and finally an EOM-CCSD calculation for the ionization potential [IP, E(N -1) – E(N)] and the electron affinity [EA, E(N + 1) - E(N)], where E(N) is (formally) the ground state energy of a system with N electrons. The band gap is the sum [IP+EA, E(N + 1) + E(N - 1) - 2E(N)]. The total cost is dominated by the ground-state CCSD calculation, which has $O(N_{\nu}^4 o^2 v^4)$ scaling in CPU time and $O(N_b^3 o^2 v^2)$ scaling in storage, where N_k is the number of k-points sampled in the Brillouin zone and o, v are the number of occupied and virtual (unoccupied) orbitals per k-point. These relatively high CPU and storage costs necessitate composite corrections and extrapolations to make predictions in the complete basis set limit and thermodynamic limit (TDL).

¹⁾Department of Chemistry, Columbia University, New York, NY 10027 USA

²⁾Department of Chemistry and Biochemistry, University of California, Santa Cruz, CA 95064 USA

a) Electronic mail: t.berkelbach@columbia.edu

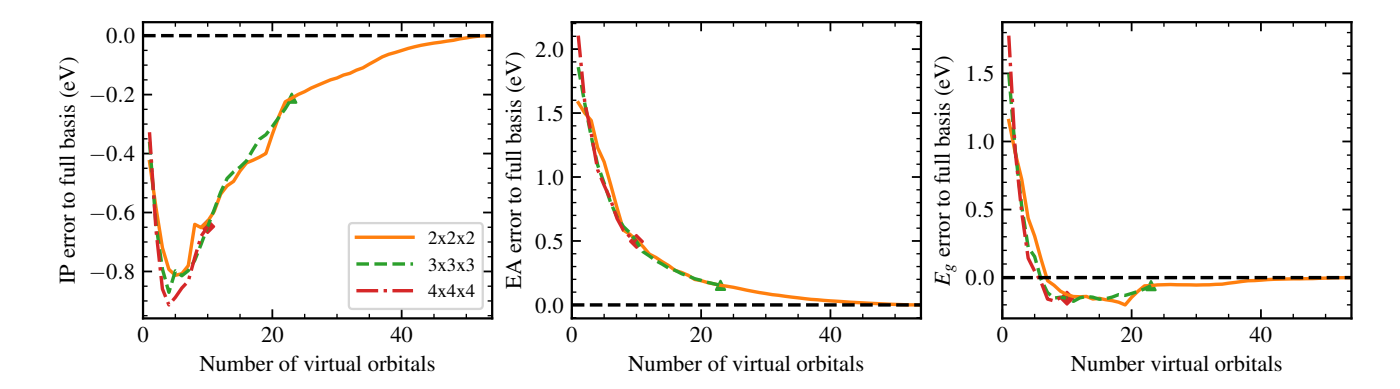


FIG. 1. Convergence of the IP, EA, and band gap with the number of correlated virtual orbitals for silicon. For $N_k = 2^3$ data, the error is defined with respect to the full TZ basis value (with 54 virtual orbitals per k-point). The $N_k = 3^3$ and 4^3 data have been shifted to align with that of the smaller k-point mesh at the largest accessed number of virtual orbitals, which is 23 for 3^3 and 10 for 4^3 .

We use GTH pseudopotentials optimized for Hartree-Fock calculations^{34,35} and the recently developed correlation consistent GTH-cc-pVTZ basis set.³⁰ Separate testing (not shown) with the QZ basis set confirm that basis set incompleteness errors due to our use of the TZ basis set are less than 0.1 eV in band gaps. We sample the Brillouin zone using uniform k-point meshes with $N_k = 2^3$, 3^3 , and 4^3 . For the larger k-point meshes, prohibitive storage costs require that we freeze virtual orbitals [we always correlate all occupied (valence) orbitals, of which there are 4 per unit cell for all materials studied here except LiH (1 occupied orbital) and AlN (8 occupied orbitals)]. We thus use a composite correction based on calculations with smaller N_k ,

$$E(N_{k2}, L) \approx E(N_{k2}, S) + [E(N_{k1}, L) - E(N_{k1}, S)]$$
 (1)

where L and S indicate a large and small number of active virtual orbitals and $N_{k,2} > N_{k,1}$. For $N_k = 2^3$, we correlate the entire TZ basis set (except for AlN), which contains between 34 and 58 (67 for truncated AlN) orbitals per k-point; for $N_k = 3^3$, we correlate 27 total orbitals per k-point and correct based on calculations with $N_k = 2^3$; for $N_k = 4^3$, we correlate 14 total orbitals per k-point and correct based on calculations with $N_k = 3^3$. Therefore, our calculations treat a few hundred electrons in about 1000 total orbitals, but benefit from the savings implied by the translational symmetry of solids.

In Fig. 1, we show the convergence of the (composite corrected) IP, EA, and band gap as a function of the number of virtual orbitals, using silicon as an example. We see that the shape of convergence for all N_k is quite similar, suggesting that the composite corrections are accurate. The IP and EA have large, but opposite, frozen orbital errors; these errors cancel in the band gap, which converges to within 0.2 eV when correlating only 10 virtual orbitals per k-point and to within 0.1 eV when correlating 23 virtual orbitals per k-point. Beyond about 10 virtual orbitals, we see that the band gap converges from below, which is a general trend seen in most other materials.

With these basis-set corrected estimates, we use a two-point extrapolation to the TDL assuming finite-size errors that de-

cay as $N_{k}^{-1/3}$,

$$E(N_k \to \infty) \approx \frac{N_{k,2}^{1/3} E(N_{k,2}) - N_{k,1}^{1/3} E(N_{k,1})}{N_{k,2}^{1/3} - N_{k,1}^{1/3}},$$
 (2)

where $N_{k,2} = 4^3$ and $N_{k,1} = 3^3$. This slow convergence with N_k is attributable to the finite-size error of a charged unit cell and is shared by most many-body methods.³⁶

In Fig. 2, we demonstrate this composite correction and extrapolation scheme for four example solids: Si, BN, MgO, and LiH. As already mentioned, we see that increasing the number of correlated orbitals increases the band gap. We see that the difference in band gaps when correlating 27 or 14 orbitals is relatively independent of N_k (at least for $N_k = 2^3$ and 3^3), indicating that our additive composite correction should be accurate. For any given N_k , we estimate that our band gaps are basis-set converged to within about 0.1 eV, although extrapolation can magnify these individual errors. Moreover, the final basis-set corrected data (with $N_k = 2^3$, 3^3 , and 4^3) do not always fall on a straight line, suggesting that we may not have reached the limit where the finite-size error is exclusively due to the leading-order term of $O(N_k^{-1/3})$.

C. P-EOM-MP2 calculations

Because of the high cost of periodic EOM-CCSD calculations, it is worthwhile to compare to more affordable theories such as MP2, i.e., the calculation of IPs, EAs, and band gaps using the second-order self-energy with a Hartree-Fock reference. However, MP2 has been shown to perform poorly for band gaps, predicting negative band gaps for semiconductors like silicon. The semiconductors like silicon. Instead, our group recently explored the accuracy of the closely related partitioned EOM-MP2 (P-EOM-MP2) theory. In P-EOM-MP2, we make two approximations to an EOM-CCSD calculation. First, we replace the ground-state CCSD amplitudes by their second-order approximations. Second, we replace the large doubles-doubles block of the similarity transformed Hamiltonian by a diagonal ma-

trix, keeping only the orbital energy differences. These approximations lower the CPU and memory costs significantly.

A diagrammatic analysis in Ref. 39 showed that a P-EOM-MP2 calculation essentially corresponds to supplementing the second-order self-energy with two third-order diagrams. Remarkably, this minor difference resulted in significantly improved performance. In this work, we will compare our EOM-CCSD results to P-EOM-MP2 results, which have been recalculated here for consistency with the pseudopotentials, basis sets, and *k*-points used in this work. However, we find numbers in good agreement with our previous work,³⁹ suggesting that errors due to these latter technical details are small.

III. RESULTS

A. Comparing EOM-CCSD and P-EOM-MP2

Before comparing to experimental band gaps, we first compare the performance of EOM-CCSD and P-EOM-MP2. In Fig. 3, we compare the (composite corrected) band gaps as a function of N_k for four example materials. Clearly, for many materials, the calculated band gaps are very similar: at fixed N_k , the gaps commonly differ by less than 0.2 eV, which is a significant finding given the difference in cost between the two methods.

However, for silicon (and a few other materials, see below), we see large differences that are magnified on approaching the TDL. With $N_k = 4^3$, the EOM-CCSD gap is smaller by 0.4 eV, and extrapolation to the TDL magnifies this difference to 1.0 eV. We note that our EOM-CCSD band gap in the TDL is

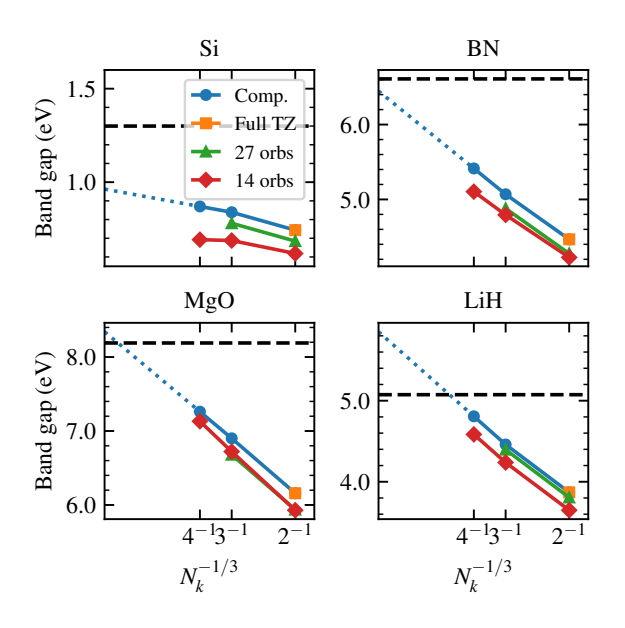


FIG. 2. Behavior of the band gap as function of N_k when correlating the total number of orbitals indicated (14, 27, or the full TZ basis). The composite corrected curve (blue) is our best estimate of the basis set limit, which is then extrapolated to the thermodynamic limit. The black dashed line indicates the experimental band gap.

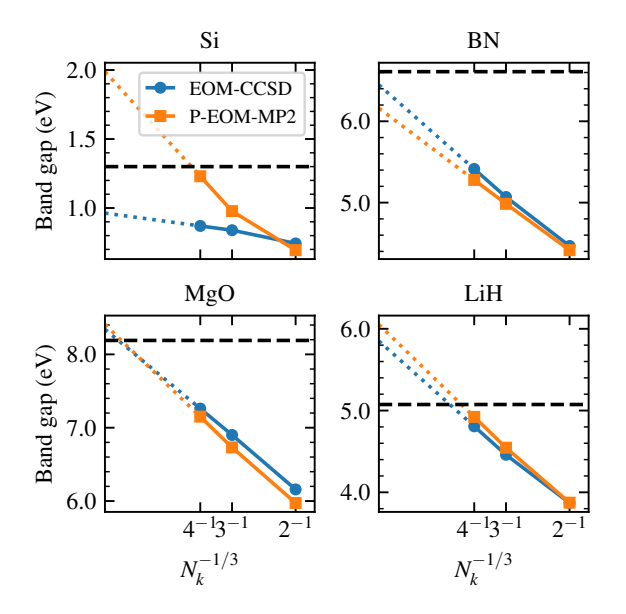


FIG. 3. Comparison of EOM-CCSD and P-EOM-MP2 band gaps upon extrapolation to the thermodynamic limit. The black dashed line indicates the experimental band gap.

0.96 eV, which is slightly smaller than the previously reported value of 1.19 eV. We have confirmed that this discrepancy is due to a combination of small errors in our composite correction and differences in our basis set, pseudopotential, and k-point used for the conduction band minimum.

We next sought to identify any trend in the difference between P-EOM-MP2 and EOM-CCSD band gaps. In Fig. 4, we show the difference of the IP, EA, and band gap as a function of the experimental band gap; because extrapolation sometimes alters the difference, we show differences at $N_k = 4^3$ and in the extrapolated TDL. We identify the following rough trends. The P-EOM-MP2 IP is larger for small gap materials and smaller for large gap materials; the P-EOM-MP2 EA is larger for most materials; the P-EOM-MP2 band gap is larger for most materials (typically by less than 0.5 eV), but similar for large gap materials. The similarity of the band gaps for large materials is consistent with their more weakly correlated nature. Overall, we find that P-EOM-MP2 and EOM-CCSD predict surprisingly similar band gaps. The largest outliers occur for small gap materials upon extrapolation, and these are Si and BP, for which P-EOM-MP2 predicts a band gap that is larger by about 1 eV.

B. Comparing to experiment

We now turn to a comparison between calculated and experimental band gaps. Our basis-set corrected and TDL extrapolated results for the electronic band gap are given in Tab. I, where they are compared to experimental band gaps. For a fair comparison, we have corrected the experimental band gaps for finite-temperature and vibrational zero-point energy effects, which typically act to reduce the purely electronic

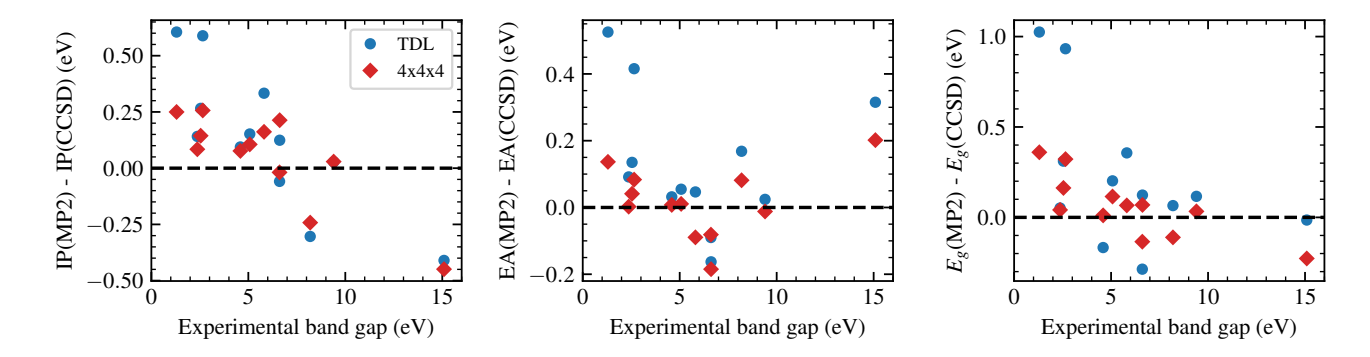


FIG. 4. Difference between P-EOM-MP2 and EOM-CCSD for the IP, EA, and band gap E_g of all materials studied in this work. Differences are shown for values calculated with a $4 \times 4 \times 4$ k-point mesh and for values extrapolated to the thermodynamic limit (TDL).

Material	a (c) (Å)	Reference		P-EOM-MP2		EOM-CCSD	
		Expt. $E_{\rm g}$ (corrected)	el-ph	$E_{ m g}$	Error	$E_{ m g}$	Error
Si	5.431	1.30	-0.06	1.99	0.69	0.96	-0.34
SiC	4.350	2.37	-0.17	2.59	0.22	2.54	0.17
AlP	5.451	2.54^{40}	-0.09	2.93	0.39	2.62	0.08
BP	4.538	2.65	-0.25^{41}	2.58	-0.07	1.65	-1.00
MgS	5.191	4.59 ⁴²	_	5.10	(0.51)	5.26	(0.67)
LiH	4.083	5.07^{43}	-0.08^{44}	6.05	0.98	5.85	0.78
C	3.567	5.81	-0.33	5.24	-0.57	4.88	-0.93
BN	3.615	6.61	-0.41	6.16	-0.45	6.45	-0.16
AlN	3.110 (4.980)	6.62	-0.42	6.45	-0.17	6.33	-0.29
MgO	4.213	8.19	-0.52	8.41	0.22	8.34	0.15
LiCl	5.130	9.40^{45}	_	9.55	(0.15)	9.43	(0.03)
LiF	4.035	15.09	-0.59	15.41	0.32	15.43	0.34
MSE (eV)					0.16		-0.12
MAE (eV)					0.41		0.42

TABLE I. Lattice constants and electronic band gaps of the 12 materials studied in this work (all energies in eV). Experimental band gaps have been corrected for the effects of electron-phonon coupling, when such corrections are available in literaure. Except where indicated, experimental band gaps have been taken from the collection in Ref. 46, and electron-phonon corrections have been taken from the collection in Ref. 39.

band gap. If we exclude solids without available electronphonon corrections, EOM-CCSD predicts band gaps with a mean signed error (MSE) of -0.12 eV and a mean absolute error (MAE) of 0.42 eV. The largest outliers are diamond (error of -0.93 eV), BP (-1.00 eV), and LiH (+0.78 eV). The statistical performance of P-EOM-MP2 is quite similar, with an MSE of 0.16 eV and MAE of 0.41 eV.

The performance of both methods is shown graphically in Fig. 5, along with that of two other Green's function based methods, whose band gaps were previously published: the extended second-order algebraic diagrammatic construction $[ADC(2)-X]^{47}$ and the G_0W_0 approximation with a PBE reference. We choose these two for comparison because their calculations were also performed with PySCF, using similar basis sets and pseudopotentials. We see that EOM-CCSD and P-EOM-MP2 outperform ADC(2)-X, which predicts band gaps that are too small, but are comparable to the G_0W_0 approximation.

IV. CONCLUSIONS

Through a study of 12 simple semiconductors and insulators, we have found that EOM-CCSD predicts band gaps with a mean absolute error of about 0.4 eV. Perhaps unsurprisingly, this accuracy is very similar to our group's previous finding concerning the accuracy of EOM-CCSD for neutral excitation energies of solids. ^{24,25} Overall, we conclude that the performance of EOM-CCSD is not measurably better than that of P-EOM-MP2, even for small gap semiconductors that one might expect to be more strongly correlated.

Although we believe our results are converged (with respect to basis set and number of k-points) to about $0.1-0.2~{\rm eV}$, the need for composite corrections and extrapolation introduces uncertainties and prevents routine use of these correlated methods. More robust methods for the reduction of basis set errors and finite-size errors would be very valuable. Having established the performance of band gaps of simple solids, future work should explore more complex solids as well as core ionization energies and the charged excitations of metals. The degree to which EOM-CCSD can replace or

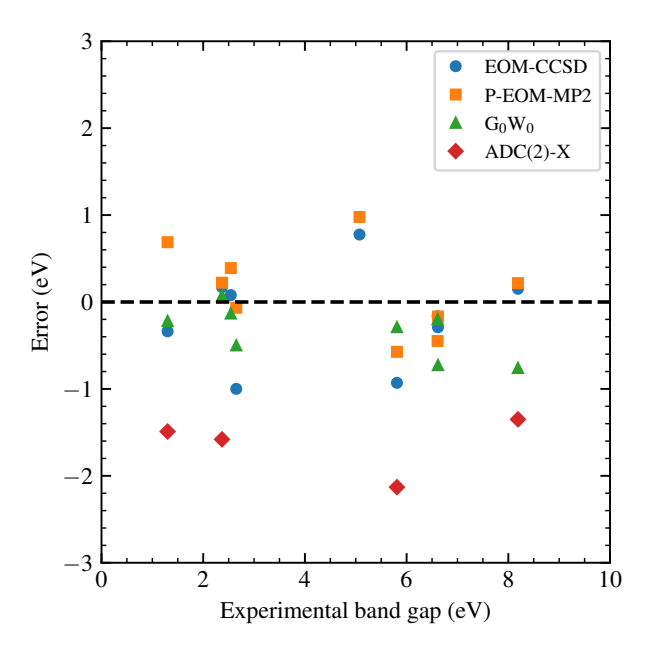


FIG. 5. Band gap error for the 12 semiconductors and insulators studied in this work. In addition to our own EOM-CCSD and P-EOM-MP2 results, we include ADC(2)-X results⁴⁷ and G_0W_0 results⁴⁶ from previous works, for comparison; only some of the same solids were studied in these previous works.

complement existing and more affordable methods remains to be seen. Predicting very precise excitation energies through the incorporation of full or perturbative triples—a manner of systematic improvability that is not shared by most existing methods—is perhaps the most exciting near-term goal. Addressing the cost is the outstanding challenge.

¹J. P. Perdew, "Density functional theory and the band gap problem," Int. J. Quantum Chem. **28**, 497–523 (1986).

²A. Seidl, A. Görling, P. Vogl, J. A. Majewski, and M. Levy, "Generalized kohn-sham schemes and the band-gap problem," Phys. Rev. B **53**, 3764–3774 (1996).

³P. Mori-Sánchez, A. J. Cohen, and W. Yang, "Localization and delocalization errors in density functional theory and implications for band-gap prediction," Phys. Rev. Lett. **100**, 146401 (2008).

⁴J. Muscat, A. Wander, and N. Harrison, "On the prediction of band gaps from hybrid functional theory," Chem. Phys. Lett. **342**, 397–401 (2001).

⁵H. Xiao, J. Tahir-Kheli, and W. A. Goddard, "Accurate band gaps for semi-conductors from density functional theory," J. Phys. Chem. Lett. 2, 212–217 (2011).

⁶A. J. Garza and G. E. Scuseria, "Predicting band gaps with hybrid density functionals," J. Phys. Chem. Lett. 7, 4165–4170 (2016).

⁷L. Hedin, "New method for calculating the one-particle green's function with application to the electron-gas problem," Phys. Rev. **139**, A796–A823 (1965)

⁸M. S. Hybertsen and S. G. Louie, "First-principles theory of quasiparticles: Calculation of band gaps in semiconductors and insulators," Phys. Rev. Lett. 55, 1418–1421 (1985).

⁹M. S. Hybertsen and S. G. Louie, "Electron correlation in semiconductors and insulators: Band gaps and quasiparticle energies," Phys. Rev. B 34, 5390–5413 (1986).

¹⁰F. Bruneval, N. Vast, and L. Reining, "Effect of self-consistency on quasi-particles in solids," Phys. Rev. B 74, 045102 (2006).

¹¹M. van Schilfgaarde, T. Kotani, and S. Faleev, "Quasiparticle self-consistent gw theory," Phys. Rev. Lett. 96, 226402 (2006). ¹²M. Shishkin, M. Marsman, and G. Kresse, "Accurate quasiparticle spectra from self-consistent gw calculations with vertex corrections," Phys. Rev. Lett. 99, 246403 (2007).

¹³W. Chen and A. Pasquarello, "Accurate band gaps of extended systems via efficient vertex corrections in gw," Phys. Rev. B 92, 041115 (2015).

¹⁴A. L. Kutepov, "Full versus quasiparticle self-consistency in vertex-corrected GW approaches," Phys. Rev. B 105, 045124 (2022).

¹⁵C.-N. Yeh, S. Iskakov, D. Zgid, and E. Gull, "Fully self-consistent finite-temperature gw in gaussian bloch orbitals for solids," Phys. Rev. B 106, 235104 (2022).

¹⁶J. McClain, Q. Sun, G. K.-L. Chan, and T. C. Berkelbach, "Gaussian-based coupled-cluster theory for the ground-state and band structure of solids," J. Chem. Theory Comput. 13, 1209–1218 (2017).

¹⁷Y. Gao, Q. Sun, J. M. Yu, M. Motta, J. McClain, A. F. White, A. J. Minnich, and G. K.-L. Chan, "Electronic structure of bulk manganese oxide and nickel oxide from coupled cluster theory," Phys. Rev. B 101, 165138 (2020).

¹⁸A. Pulkin and G. K.-L. Chan, "First-principles coupled cluster theory of the electronic spectrum of transition metal dichalcogenides," Phys. Rev. B 101, 241113 (2020).

¹⁹K. Laughon, J. M. Yu, and T. Zhu, "Periodic coupled-cluster green's function for photoemission spectra of realistic solids," J. Phys. Chem. Lett. 13, 9122–9128 (2022).

²⁰T. Zhu, C. A. Jiménez-Hoyos, J. McClain, T. C. Berkelbach, and G. K.-L. Chan, "Coupled-cluster impurity solvers for dynamical mean-field theory," Phys. Rev. B 100, 115154 (2019).

²¹A. Shee and D. Zgid, "Coupled cluster as an impurity solver for green's function embedding methods," J. Chem. Theory Comput. 15, 6010–6024 (2019).

²²T. Zhu, Z.-H. Cui, and G. K.-L. Chan, "Efficient formulation of ab initio quantum embedding in periodic systems: Dynamical mean-field theory," J. Chem. Theory Comput. 16, 141–153 (2019).

²³A. M. Lewis and T. C. Berkelbach, "Ab initio linear and pump-probe spectroscopy of excitons in molecular crystals," J. Phys. Chem. Lett. 11, 2241–2246 (2020).

²⁴X. Wang and T. C. Berkelbach, "Excitons in solids from periodic equation-of-motion coupled-cluster theory," J. Chem. Theory Comput. 16, 3095–3103 (2020).

²⁵X. Wang and T. C. Berkelbach, "Absorption spectra of solids from periodic equation-of-motion coupled-cluster theory," J. Chem. Theory Comput. 17, 6387–6394 (2021).

²⁶A. Dittmer, R. Izsák, F. Neese, and D. Maganas, "Accurate band gap predictions of semiconductors in the framework of the similarity transformed equation of motion coupled cluster theory," Inorg. Chem. 58, 9303–9315 (2019).

²⁷A. Gallo, F. Hummel, A. Irmler, and A. Grüneis, "A periodic equation-of-motion coupled-cluster implementation applied to f-centers in alkaline earth oxides," J. Chem. Phys. 154, 064106 (2021).

²⁸B. T. G. Lau, B. Busemeyer, and T. C. Berkelbach, "Optical properties of defects in solids via quantum embedding with good active space orbitals," arXiv:2301.09668 (2023).

²⁹Q. Sun, T. C. Berkelbach, J. D. McClain, and G. K.-L. Chan, "Gaussian and plane-wave mixed density fitting for periodic systems," J. Chem. Phys. 147, 164119 (2017).

³⁰H.-Z. Ye and T. C. Berkelbach, "Fast periodic gaussian density fitting by range separation," J. Chem. Phys. 154, 131104 (2021).

³¹H.-Z. Ye and T. C. Berkelbach, "Tight distance-dependent estimators for screening two-center and three-center short-range coulomb integrals over gaussian basis functions," J. Chem. Phys. 155 (2021), 10.1063/5.0064151.

³²H.-Z. Ye and T. C. Berkelbach, "Correlation-consistent gaussian basis sets for solids made simple," J. Chem. Theory Comput. 18, 1595–1606 (2022).

³³Q. Sun, T. C. Berkelbach, N. S. Blunt, G. H. Booth, S. Guo, Z. Li, J. Liu, J. D. McClain, E. R. Sayfutyarova, S. Sharma, S. Wouters, and G. K.-L. Chan, "Pyscf: the python-based simulations of chemistry framework," WIREs Comput. Mol. Sci. 8, e1340 (2017).

³⁴S. Goedecker, M. Teter, and J. Hutter, "Separable dual-space gaussian pseudopotentials," Phys. Rev. B 54, 1703–1710 (1996).

³⁵C. Hartwigsen, S. Goedecker, and J. Hutter, "Relativistic separable dual-space gaussian pseudopotentials from h to rn," Phys. Rev. B 58, 3641–3662 (1998).

- ³⁶Y. Yang, V. Gorelov, C. Pierleoni, D. M. Ceperley, and M. Holzmann, "Electronic band gaps from quantum monte carlo methods," Phys. Rev. B **101**, 085115 (2020).
- ³⁷M. Marsman, A. Grüneis, J. Paier, and G. Kresse, "Second-order møllerplesset perturbation theory applied to extended systems. i. within the projector-augmented-wave formalism using a plane wave basis set," J. Chem. Phys. 130, 184103 (2009).
- ³⁸A. Grüneis, M. Marsman, and G. Kresse, "Second-order møller-plesset perturbation theory applied to extended systems. II. structural and energetic properties," J. Chem. Phys. 133, 074107 (2010).
- ³⁹M. F. Lange and T. C. Berkelbach, "Improving MP2 bandgaps with lowscaling approximations to EOM-CCSD," J. Chem. Phys. 155, 081101 (2021).
- ⁴⁰M. R. Lorenz, R. Chicotka, G. D. Pettit, and P. J. Dean, "The fundamental absorption edge of alas and alp," Solid State Commun. 8, 693-697 (1970).
- ⁴¹V.-A. Ha, B. Karasulu, R. Maezono, G. Brunin, J. B. Varley, G.-M. Rignanese, B. Monserrat, and G. Hautier, "Boron phosphide as a p-type transparent conductor: Optical absorption and transport through electron-

- phonon coupling," Phys. Rev. Materials 4, 065401 (2020). $^{42}\rm W.$ Y. Ching, F. Gan, and M.-Z. Huang, "Band theory of linear and nonlinear susceptibilities of some binary ionic insulators," Phys. Rev. B 52, 1596-1611 (1995).
- $^{\rm 43} S.$ Baroni, G. Pastori Parravicini, and G. Pezzica, "Quasiparticle band structure of lithium hydride," Phys. Rev. B 32, 4077–4087 (1985).
- ⁴⁴B. Monserrat, N. D. Drummond, and R. J. Needs, "Anharmonic vibrational properties in periodic systems: energy, electron-phonon coupling, and stress," Phys. Rev. B 87, 144302 (2013).
- ⁴⁵F. C. Brown, C. Gähwiller, H. Fujita, A. B. Kunz, W. Scheifley, and N. Carrera, "Extreme-ultraviolet spectra of ionic crystals," Phys. Rev. B 2, 2126-
- ⁴⁶T. Zhu and G. K.-L. Chan, "All-electron gaussian-based g0w0 for valence and core excitation energies of periodic systems," J. Chem. Theory Comput. **17**, 727–741 (2021).
- ⁴⁷S. Banerjee and A. Y. Sokolov, "Non-dyson algebraic diagrammatic construction theory for charged excitations in solids," J. Chem. Theory Comput. 18, 5337-5348 (2022).